Applied Catalysis B: Environmental 89 (2009) 503–509

Contents lists available at ScienceDirect

Applied Catalysis B: Environmental

journal homepage: www.elsevier.com/locate/apcatb

Carbon nanotubes/titanium dioxide ($CNTs/TiO_2$) nanocomposites prepared by conventional and novel surfactant wrapping sol–gel methods exhibiting enhanced photocatalytic activity

Bin Gao [a], George Z. Chen [b], Gianluca Li Puma [a,*]

[a] Photocatalysis & Photoreaction Engineering, Department of Chemical and Environmental Engineering, The University of Nottingham, University Park, Nottingham NG7 2RD, United Kingdom
[b] Electrochemical Technologies, Department of Chemical and Environmental Engineering, The University of Nottingham, University Park, Nottingham NG7 2RD, United Kingdom

ARTICLE INFO

Article history:
Received 18 November 2008
Received in revised form 15 January 2009
Accepted 18 January 2009
Available online 24 January 2009

Keywords:
Carbon nanotubes
Titanium dioxide
Photocatalysis
Nanocomposite
Surfactant
Wrapping
Sol–gel

ABSTRACT

In this work, a conventional sol–gel method was used to prepare $CNTs/TiO_2$ nanocomposites with different carbon loading in the range up to 20% $CNTs/TiO_2$ by weight. The bare CNTs (multi-walled), and the composites were characterized by a range of analytical techniques including TEM, XRD, BET and TGA–DSC. The results show the successful covering of the CNTs with discrete clusters of TiO_2 and bare CNTs surfaces which after annealing at 500 °C led to mesoporous crystalline TiO_2 (anatase) clusters. The photocatalytic activities of the nanocomposites were monitored from the results of the photodegradation of methylene blue (MB). The optimum $CNTs/TiO_2$ ratio in the composites prepared by conventional sol–gel method was found to be in the range from 1.5% to 5% by weight under the experimental conditions investigated. The maximum increase in activity was found to be 12.8% compared to the pure TiO_2 sample.

In contrast, the synthesis of $CNTs/TiO_2$ nanocomposites by a novel surfactant wrapping sol–gel method [B. Gao, C. Peng, G.Z. Chen, G. Li Puma, Appl. Catal. B: Environ. 85 (2008) 17.] led to a uniform and well-defined nanometer-scale titania layer on individual CNTs. The nanocomposites were found to enhance the initial oxidation rate of methylene blue by onefold compared to the pure TiO_2 sample. This larger degree of rate enhancement is attributed to the supporting role of the CNTs and surface properties prepared by this novel modified sol–gel method.

1. Introduction

Heterogeneous photocatalysis is a process in which the surface of an oxide semiconductor promotes reactions upon irradiation with photons with band-gap energy or greater. Under these conditions, valence band electrons are excited and move to the conduction band leaving behind holes. The electron and holes must then migrate to the surface of the semiconductor to promote reduction and oxidation reactions of adsorbed species or of species that are in close proximity to the surface of the semiconductor. However, electron–hole recombination, at the surface or in the bulk, competes with the above process and limits the quantum yield of photocatalytic reactions [1].

Titanium dioxide (TiO_2) (E_{bg} = 3.2 eV for anatase) has been one of the most common semiconductors studied for the oxidation or reduction of inorganic and organic species. Reactive radicals (primarily $OH^{\bullet}$ and $O_2^{-\bullet}$) or direct hole oxidation are believed to initiate the oxidation of most organic species in water and air. For an organic molecule, the process may lead to partial oxidation or can proceed toward total mineralization and formation of CO_2 and mineral acids. The overall efficiency of photon utilisation by TiO_2 is however limited by electron–hole recombination, photon scattering and the intrinsic physical properties of TiO_2 that limit the absorption of photons to those with UV-A or greater energy [2].

The coupling of TiO_2 with carbon nanotubes (CNTs) has been shown to provide a synergistic effect which can enhance the overall efficiency of a photocatalytic process. $CNTs/TiO_2$ nanocomposites have attracted attention in the literature in relation to the treatment of contaminated water and air by heterogeneous photocatalysis [3,4], hydrogen evolution [5], CO_2 photo-reduction [6], dye sensitised solar cells [7] and sensors devices [8]. The conductive structure of the CNTs scaffolds is believed to favour the separation of the photo-generated electron–hole pairs by formation of heterojunctions at the $CNTs/TiO_2$ interface [9]. TiO_2 is

* Corresponding author. Tel.: +44 115 951 4170; fax: +44 115 951 4115.
E-mail address: gianluca.li.puma@nottingham.ac.uk (G. Li Puma).

0926-3373/$ – see front matter © 2009 Elsevier B.V. All rights reserved.
doi:10.1016/j.apcatb.2009.01.009

an n-type semiconductor, however, in the presence of CNTs, photogenerated electrons may move freely towards the CNTs surface, which may have a lower Fermi level, and this leaves an excess of valence band holes in the TiO_2 to migrate to the surface and react. Therefore, effectively the TiO_2 behaves as a p-type semiconductor [10]. CNTs can provide spatial confinement of TiO_2 and large supporting surface areas, leading to faster observed rates of redox reactions. In addition, the application of anodic potentials on irradiated CNTs/TiO_2 composites films may result in a further enhancement [11].

CNTs/TiO_2 composite materials have been fabricated by a range of different methods including, mechanical mixing of TiO_2 and CNTs [5], sol–gel synthesis of TiO_2 in the presence of CNTs [3], electro-spinning methods [12,13], electrophoretic deposition [14] and chemical vapour deposition [9]. The uniformity of the oxide coating and the physical properties of the composite materials vary according to the preparation method. Though uniform coating of TiO_2 on CNTs may be achieved by chemical vapour deposition and electro-spinning methods [9,12,13], these techniques are somehow not simple, require specialised equipment and it may not be easy to quantify the ratio between composite compounds. Sol–gel methods are still preferred, although they usually lead to a heterogeneous, non-uniform coating of CNTs by TiO_2, showing bare CNTs surfaces and random aggregation of TiO_2 onto the CNTs surface [3,15,16]. A few exceptions are the works by Jitianu et al. [17,18] and Zein and Boccaccini [19].

Recently, we have demonstrated the feasibility of a novel surfactant wrapping sol–gel method for coating a uniform and well-defined nanometer-scale TiO_2 layer on individual CNTs (multi-walled), producing a mesoporous anatase nanocomposite film [11]. In this work, we investigate the characteristics of CNTs/TiO_2 nanocomposites prepared by a conventional sol–gel method and we evaluate their activity towards the photocatalytic degradation of a model organic substance (methylene blue) in aqueous suspensions. Furthermore, we demonstrate that the preparation of CNTs/TiO_2 nanocomposites by the surfactant wrapping sol–gel method [11] yields nanocomposites exhibiting much higher activity compared to the samples prepared by a conventional sol–gel method, and a onefold rate enhancement with respect to TiO_2 alone.

2. Experimental

2.1. Acid treatment of CNTs

Acid treatment of carbon nanotubes was used to improve the solubility of CNTs in water by functionalisation of the nanotube surfaces with anionic groups. The treatment could also lead to opening of the ends and/or breakage of the tubes and removal of amorphous carbon and metal catalyst.

Multi-walled carbon nanotubes (MWNTs), 10–30 nm in diameter and 5–15 μm in length, were purchased from Shenzhen Nanotech Port Co., Ltd., China. Aqueous solutions were prepared with Millipore grade water. In a typical acid treatment, 1 g CNTs was mixed with a 40 ml acid mixture of concentrated sulphuric acid (Parmacos, 97–99%) and nitric acid (VWR BDH Prolabo, 69%) with a volume ratio of 3:1 [20,21]. Ultrasonication (10 min) was performed to disperse the CNTs in the suspension and to improve the contact between the nanotubes surface and the oxidant molecules. The mixture was then heated to 140 °C (the boiling point of the mixture) for 20 min under refluxing and cooled naturally to room temperature (25 °C). A longer reflux time was found to cause serious fractionation and even damage to the tubular structure of the nanotubes. The solution was then sonicated for 20 min, diluted with deionised water and filtered through a grade four fritted ceramic disc. The layer deposited on the filter was washed with deionised water until the pH of the filtered solution was about 6–7. The product was then dried at 60 °C in an oven and kept in a desiccator for further use.

2.2. Synthesis of CNTs/TiO_2 nanocomposite by a conventional sol–gel method

In a conventional sol–gel synthesis of CNTs/TiO_2 nanocomposite, the acid treated CNTs were added to provide a weight ratio of CNTs over TiO_2 in the range from 1.5% to 20%, indicated with C_{CNTs}. They were then dispersed into a 30-ml solution containing 2.7 ml water and 27.3 ml isopropanol (Fluka, puriss), under sonication which lasted 1 h. The titanium precursor solution, 3.41 ml titanium isopropoxide (Fluka, purum) in 18 ml isopropanol was added dropwise into the CNTs suspension under vigorous stirring. The mixture was left at room temperature under stirring for 2 h to complete the hydrolysis reaction. The solution was then filtered and washed with ethanol and water for three cycles and dried at 100 °C for 1.5 h. The CNTs/TiO_2 solids were ground into a powder and stored in a dessicator for further usage. A control sample was also prepared following the above method but in the absence of CNTs. The samples were sintered at 500 °C for 30 min to obtain crystalline TiO_2 in the nanocomposites.

2.3. Synthesis of CNTs/TiO_2 nanocomposite by the surfactant wrapping sol–gel method

CNTs/TiO_2 nanocomposites were also synthesised following the surfactant wrapping sol–gel method presented in our previous work [11]. In a typical synthesis of CNTs/TiO_2 nanocomposite, 35 mg of acid treated (or raw) CNTs were initially mixed with 0.5 wt.% sodium dodecylbenzenesulfonate (Aldrich) in aqueous solution. The suspension was then treated by sonication overnight to obtain a stable solution with a high weight fraction of CNTs. Under these conditions, surfactant molecules assemble on the surface of individual nanotubes with the alkyl chain groups lying flat along the tube length. The prepared CNTs solution was then dispersed in 20 ml ethanol by stirring and mixed for 30 min to reach a uniform suspension (Solution I). A predetermined amount of titanium isopropoxide (TTIP, Fluka, purum) was mixed with 15 ml ethanol (Fisher, AR Grade) and glacial acetic acid (Fisher, aldehyde free) under stirring, which was kept for 30 min to form a clear solution (Solution II). Solution II was then added dropwise into Solution I under vigorous stirring and the mixture was left at room temperature under stirring for 2 h to complete the reaction. At this stage of the synthesis procedure the Ti metal cations are captured by the negatively charged CNTs surface. A diluted ammonia solution (Fisher, 35%, S.G. 0.88) was then added dropwise to hydrolyse the residual precursor (pH 9), leading to a uniform TiO_2 coating on the CNTs surface. 10 ml ethanol was added into the reaction system and stirring was maintained for another 30 min. The suspension was centrifuged and washed with ethanol by three consecutive cycles. The final precipitate was dried in an oven at 60 °C for 10 h to obtain a powder product. The catalyst was calcined at 500 °C for 30 min to crystallize the TiO_2.

2.4. Sample analyses

The bare CNTs and the composites were characterized by a range of analytical techniques. The degree of crystallinity of the CNTs/TiO_2 composites was characterized by powder X-ray diffraction (XRD). The XRD patterns with diffraction intensity versus 2θ were recorded in a Philips EXPERT θ–2θ X-ray diffractometer with Cu Kα radiation (α = 1.54060 Å) from 10° to 80° at a scanning speed of 0.02°/s. X-ray tube voltage and current were set at 40 kV and 40 mA, respectively. The crystallite size was

estimated from the line broadening of anatase TiO_2 (2 0 0) reflection plane (2θ = ca. 48.1°), where there is negligible interference from CNTs. Nitrogen sorption isotherms and textural properties of the materials were determined in a conventional volumetric technique at 77 K using nitrogen by a Micrometrics ASAP 2010 sorptometer. Before analysis, the samples were oven-dried at 60 °C and evacuated overnight under vacuum. The sample surface area was calculated using the Brunauer–Emmett–Teller (BET) method based on adsorption data in the partial pressure (P/P_0) range of 0.05–0.35. The total pore volume was determined by the amount of nitrogen adsorbed at P/P_0 = 0.995. The average pore size was obtained from the adsorption data by Barrett–Joyner–Halenda (BJH) method. Thermogravimetric and differential scanning calorimetry analyses (TGA–DSC) were performed by a Hiden TA Q600 SDT analyzer with a heating rate of 10 °C/min under air environment with flow rate = 100 ml/min. Transmission electron microscopy (TEM) was carried out on a JEM-2010F at 200 kV. The specimens for TEM imaging were prepared by suspending solid samples in ethanol with 15 min ultrasonication and placing a drop of this mixture on a 3.05-mm diameter copper mesh (300 lines/in. mesh), which was then dried in air.

2.5. Catalyst activity tests

The photocatalytic activities of the nanocomposites were monitored from the results of the photodegradation of methylene blue (MB) (Aldrich) (10 mg/L initial concentration in a 200-ml aqueous suspension containing 0.1 g/L of catalyst). The reactions were carried out for 3 h under stirring in a Pyrex circular vessel. The reactor was irradiated by three UV-A lamps (Philips TL 8W/08 F8T5/BLB, 0.0155 m bulb diameter, 0.26 m bulb length and 1.2 W UV-A output) located directly above the vessel at a distance of 6 cm from the surface of the liquid. The lamps emitted a minute fraction of the total radiation at 324 and 325 nm and the rest between 342 and 400 nm with a maximum irradiance peak at 365 nm. The lamp axes were separated by 3 cm. The average incident photon flux (from 324 to 384 nm) at the free surface of the liquid was 24 W/m^2. The concentration of MB in the samples collected at regular intervals was measured by a Shimadzu UV-mini-1240 UV–vis spectrophotometer.

3. Results and discussion

3.1. Characterisation of CNTs/TiO_2 nanocomposites prepared by a conventional sol–gel method

TGA–DSC analysis was carried out to estimate the carbon nanotube content of the composites. The results of weight loss and heat flow as a function of temperature for raw CNTs, TiO_2 and CNTs/TiO_2 composite (10%) are shown in Fig. 1. The weight ratio of CNTs over TiO_2 was estimated by correlating the mass loss with temperature through the interpretation of the derivative of the weight loss. For the CNTs/TiO_2 composite (10%), the weight loss due to the combustion of the CNTs in the composites extends from 84.4 wt.% the point with the lowest first derivative to 74.6 wt.% the plateau achieved just after 600 °C. The results shown in Table 1 suggest that the CNTs/TiO_2 ratios estimated before the synthesis of the nanocomposites were in close agreement with the results obtained from TGA–DSC analyses. Therefore, negligible losses of CNTs occurred during the composite preparation procedure. The combustion point of CNTs in the composite was found to be 540 °C, which was determined at the temperature with the highest rate of mass loss. Conversely, the acid treated CNTs could not be combusted until approximately 700 °C (Fig. 1a). This shift may be ascribed to the presence of the metal oxide grafted on the sidewall of CNTs which may

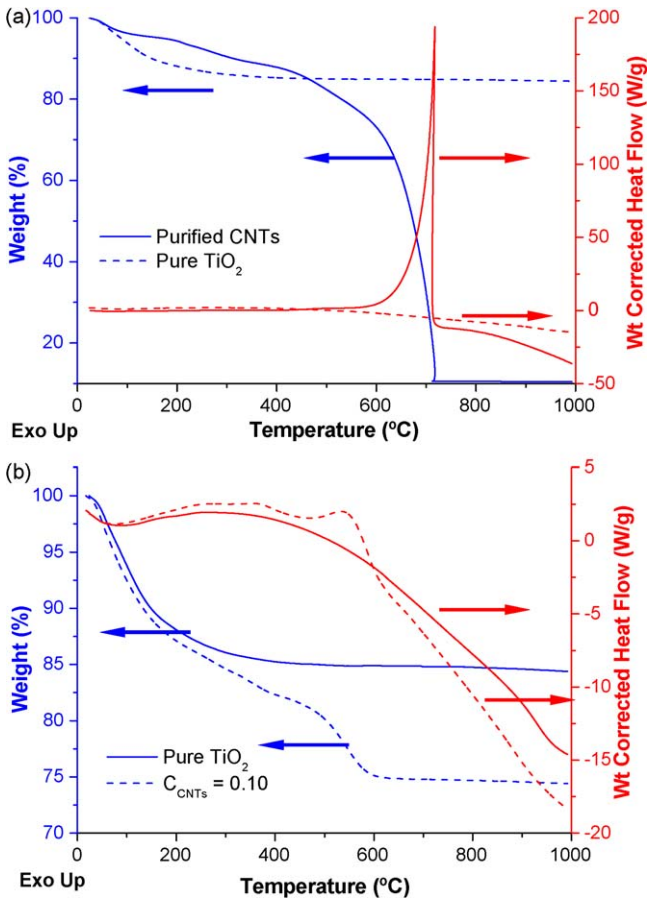

Fig. 1. TGA–DSC curves of (a) acid treated CNTs and pure TiO_2 and (b) pure TiO_2 and CNTs/TiO_2 composite (10% CNTs content).

provide the oxygen required by the reaction and/or restrain the heat transfer creating localised hot spots, facilitating the oxidation of carbon. The early fall in the DSC curve of CNTs/TiO_2 composite was due to water evaporation, followed by a little rise corresponding to the decomposition of organic residue and/or the early oxidation of purified CNTs. Moreover, it should be noted that neither TiO_2 alone nor the composite showed a distinct exothermic peak corresponding to the formation of anatase TiO_2 in the DSC curves (Fig. 1). This may suggest that restricted particle growth occurred during the sintering.

Fig. 2 shows TEM images of amorphous samples of TiO_2 alone and of CNTs/TiO_2 nanocomposites with CNTs/TiO_2 ratios of 0.015, 0.05 and 0.2 by weight. The images reveal a composite microstructure made of TiO_2 agglomerates with embedded CNTs confirming the intimate contact between the CNTs and TiO_2. However, the distribution of the clusters is far from being homogenous. The aggregation of TiO_2 nanoparticles indicates the supporting role of the CNTs as centers for the deposition and growth of hydrolysis products, as well as, the support for spatial confinement of the TiO_2 clusters. In particular, the appearance of

Table 1
Carbon contents in composites.

Carbon contents	Weight ratio of CNTs over TiO_2 in the composites (%)				
C_{ES}	1.5	3	5	10	20
C_{TG}	1.18	3.10	4.69	9.80	20.67

Notes: The carbon contents presented here correspond to the predetermined values before sample fabrication (C_{ES}) and those determined by TGA–DSC analysis (C_{TG}), respectively.

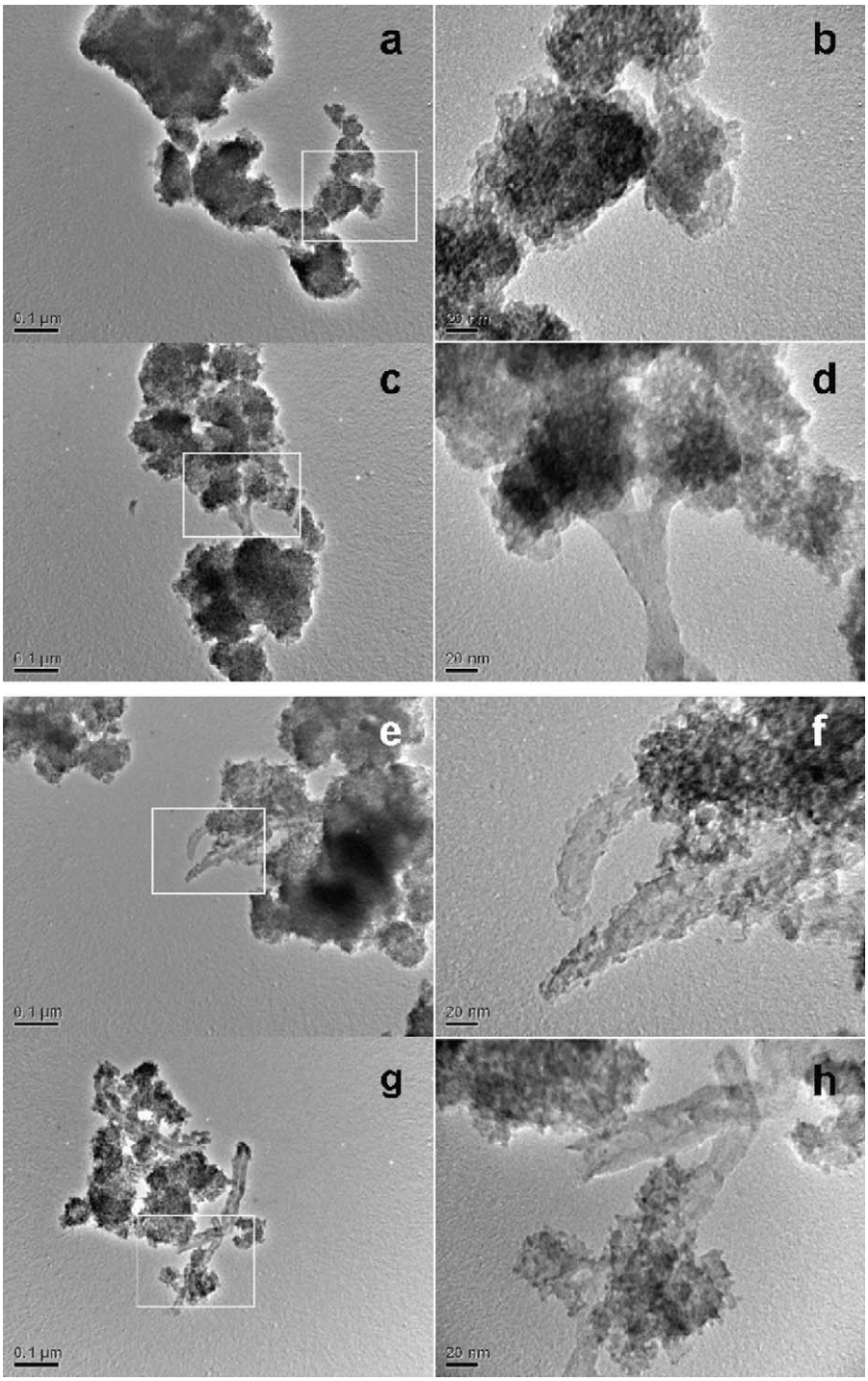

Fig. 2. TEM images of (a and b) pure TiO_2 produced without the presence of CNTs; (c–h) fresh prepared CNTs/TiO_2 nanocomposites by conventional sol–gel method with different carbon contents which are 0.015 (c and d), 0.05 (e and f) and 0.20 (g and h), respectively. Figures on the right have higher resolutions.

clear surface TiO_2 roughness on the nanotubes, shown in Fig. 2f, may also be related to the enhanced photocatalytic activity of this sample as discussed in Section 3.3. Furthermore, it can be noted that most of the TiO_2 clusters are located at the open ends of the tubular structure, suggesting the presence of functional groups on the CNTs sidewall of purified CNTs.

XRD spectra (Fig. 3) were performed to investigate the effect of carbon content on the crystallization of different samples. The patterns of the sintered composites suggested the formation of pure anatase crystallites. No characteristics peaks of CNTs were found in the spectra of the composites in the range investigated. This may be attributed to the overlap of the intense peaks of the CNTs (0 0 2) and anatase (0 0 1) reflections, as the difference in mass between CNTs and TiO_2 is relatively large.

N_2 adsorption–desorption isotherms of the composites are shown in Fig. 4. All the isotherms could be classified as type IV category, indicating the presence of capillary condensation in the mesoporous structure. In contrast with the findings of other researchers [3], the isotherms of the composites in this study exhibit a clear double-section of hysteresis between their adsorption and desorption branches, which may be regarded as an overlap of H1 and H3 loops. Such profile of the isotherms

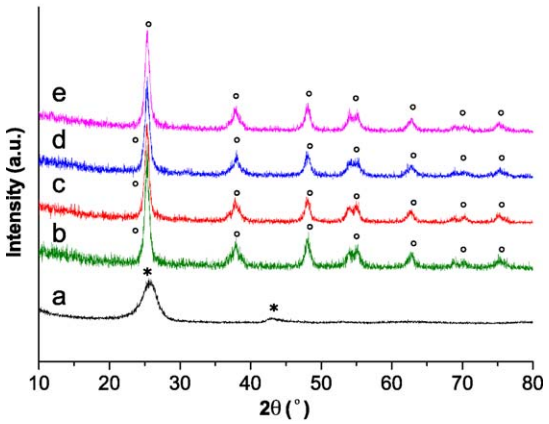

Fig. 3. X-ray diffraction patterns of purified CNTs (a), calcined pure TiO_2 (b) and CNTs/TiO_2 composites with a carbon content of 0.015 (c), 0.05 (d) and 0.20 (e). The annealing was carried out at 500 °C for 30 min. The peaks with "○"and "*" marks correspond to anatase phase TiO_2 and CNTs, respectively.

can be an indication of pore mixture comprising of mesopores and large cavities. The formation of such distinct loops may be related to the composite microstructure showing uncovered tubular bodies with large TiO_2 clusters at the ends, as seen in Fig. 2. The H1 loop is normally accredited to the presence of relatively high pore size homogeneity and a simple pore network. In contrast, the H3 loop is commonly found in the situation of loose assemblages of particles leading to slitlike pores. This can be explained in terms of the random aggregations of TiO_2/CNTs particle matrice.

Table 2 shows the anatase crystal sizes estimated by XRD and the surface properties of the composites by BET of catalyst samples with different CNTs/TiO_2 ratios. The presence of the CNTs in the nanocomposites hinders particle growth, resulting in a slight decrease of crystal size. Further increase of the carbon content in the composites shows a moderate increase in the TiO_2 crystal size, which may be due to the rapid hydrolysis of the titanium precursor before or while the reaction products anchor on the nanotubes support.

The reduction in pore volume of the composite compared to the acid treated CNTs, strongly suggested the existence of surface blockage on the CNTs. Conversely, the presence of CNTs in the composite increases surface properties (surface area, pore volume of calcined composite) compared to TiO_2 alone, confirming the supporting role of the nanotubes. The surface area enhancement of the sintered nanocomposites with increasing CNTs content may be assigned to the larger fraction of bare CNTs surfaces resulting from sample calcination. The decrease in surface area of the samples with 10% and 20% CNTs may be due to the formation of smaller TiO_2 clusters on the surface of the nanotubes (see Fig. 2g) resulting in a higher degree of coverage of the nanotubes. Therefore, the contribution of the bare CNTs surface to the total surface area diminishes in these samples.

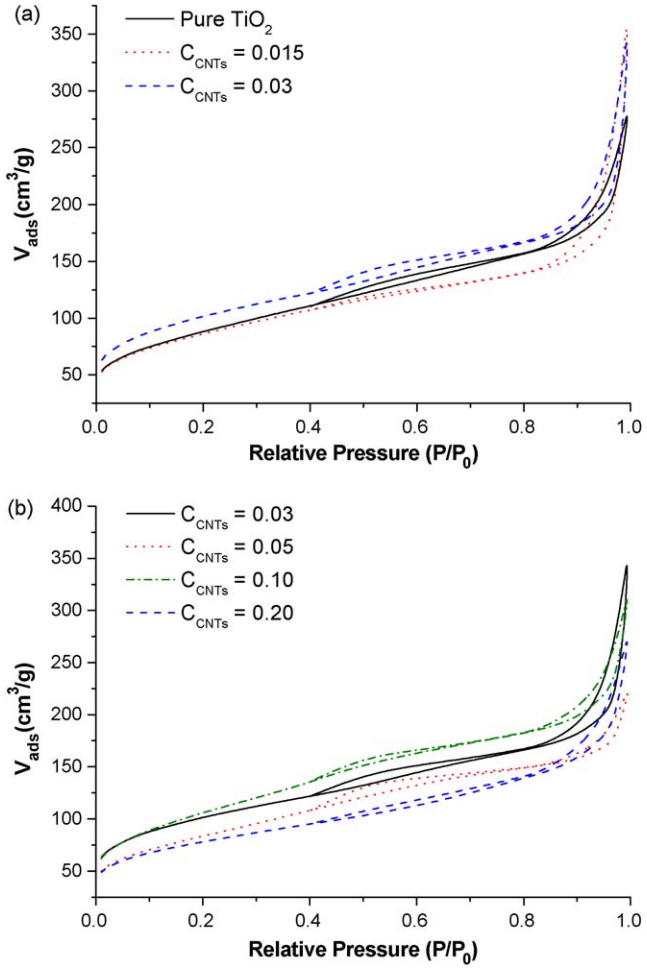

Fig. 4. N_2 adsorption–desorption isotherms of pure TiO_2 and un-calcined CNTs/TiO_2 nanocomposites with carbon content indicated.

3.2. Characterisation of CNTs/TiO_2 nanocomposite prepared by the surfactant wrapping sol–gel method

The full characterisation of CNTs/TiO_2 nanocomposites prepared by the surfactant wrapping sol–gel method with pristine CNTs (in the absence of acid treatment), including TGA–DSC, TEM, SEM, BET and XRD, has been presented elsewhere [11]. Fig. 5 compares TEM images of CNTs/TiO_2 nanocomposites prepared using pristine CNTs (a and b), and acid treated CNTs (c and d). In contrast with the sample prepared by the conventional sol–gel method (Fig. 2), the carbon nanotubes were covered uniformly with a thin layer of TiO_2. The thickness of the layer was estimated to be 5–10 nm. The composites prepared from acid treated CNTs show significant fractionalization of the tubular structure. BET analyses [27] showed that the mesoporous structure of the samples [11], with large non-filled pores between the tubes, was

Table 2
Composite crystal sizes and surface properties of catalysts.

C_{CNTS} (wt.%)	0	1.5	3	5	10	20	100
d_{TiO_2} (nm)	15.3	14.0	14.0	14.4	14.6	14.7	–
S_{BET} (m^2/g)	304.9	295.0	338.4	294.6	369.5	262.6	381.1
V_{pore} (cm^3/g)	0.297	0.269	0.308	0.260	0.337	0.275	0.754
S'_{BET} (m^2/g)	78.97	83.42	86.39	105.87	85.37	97.61	–
V'_{pore} (cm^3/g)	0.133	0.151	0.151	0.196	0.149	0.182	–

Notes: [a] d_{TiO_2} is the calculated TiO_2 crystal size from XRD spectra of calcined samples and [b] S_{BET} and V_{pore} correspond to the BET surface area and pore volume of the un-calcined sample at a relative pressure of 0.995 for N_2 at 77 K, respectively, while S'_{BET} and V'_{pore} refer to the properties after sintering.

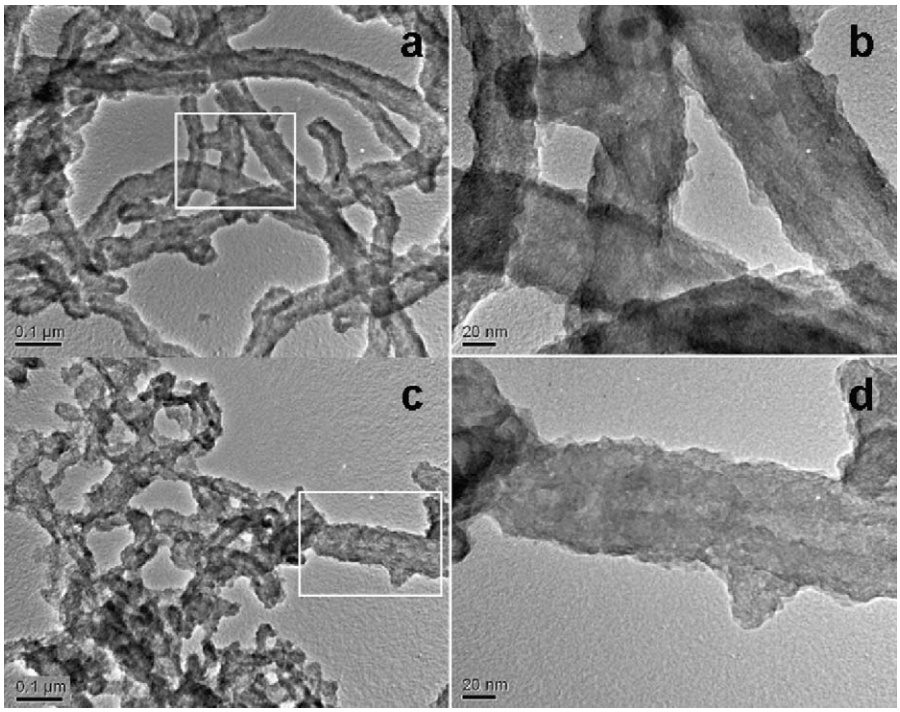

Fig. 5. TEM images of CNTs/TiO_2 nanocomposites prepared by the surfactant wrapping sol–gel method using pristine CNTs (a and b), and acid treated CNTs (c and d). (b) and (d) are the enlarged images. The CNTs to TiO_2 mass ratio is 0.9 for both samples.

retained in the samples prepared with acid treated CNTs. However, a slight increase in the surface properties (surface area and pore volume, not shown) was observed in the samples prepared with acid treated CNTs, which corroborate with the microscopy images in Fig. 5.

3.3. Photocatalytic activity of CNTs/TiO_2 nanocomposites prepared by a conventional sol–gel method

Control experiments showed that UV-A irradiation with no catalyst and catalyst (composite or pure TiO_2) without irradiation could not degrade methylene blue. Fig. 6 shows the results of the decomposition of methylene blue under irradiation, in the presence of TiO_2 alone and with the CNTs/TiO_2 composites. The optimum CNTs/TiO_2 ratio in the composites prepared by conventional sol–gel method was found to be in the range from 1.5% to 5% by weight under the experimental conditions investigated. The maximum increase in activity was found to be 12.8% compared to the pure TiO_2 sample. The sample at 10% loading was found to have activity comparable to that of pure TiO_2 (results not shown for clarity). A significant decrease in activity was observed at higher CNTs loadings (20%). The increase in activity of the CNTs/TiO_2 nanocomposites in comparison with the sample made by TiO_2 alone can be attributed to the combined effect of several possible concomitant factors: (i) the higher surface area of the composites (Table 2) providing a higher adsorption capacity of reactive species [4]; (ii) the formation of CNTs/TiO_2 heterojunctions which could reduce the rate of the recombination of photoinduced electrons and holes [9]; (iii) the possible shift of the apparent Fermi level to more positive values of the CNTs/TiO_2 nanocomposites as compared to pure TiO_2 [22] therefore allowing the utilisation of longer wavelength photons (note that the emission spectrum of the UV-A lamps extends to 400 nm) although the verification remains a challenge because of the presence of CNTs; (iv) the absorption of photons by the bare CNTs surface injecting electrons into the TiO_2 conduction band and triggering the formation of reacting radicals (superoxide and hydroxyl radicals) [23]. The decrease in activity at higher CNTs loadings (10% or higher in this work) can be the results of photon scattering by the bare carbon phase, as well as, insufficient covering of the carbon nanotubes with TiO_2.

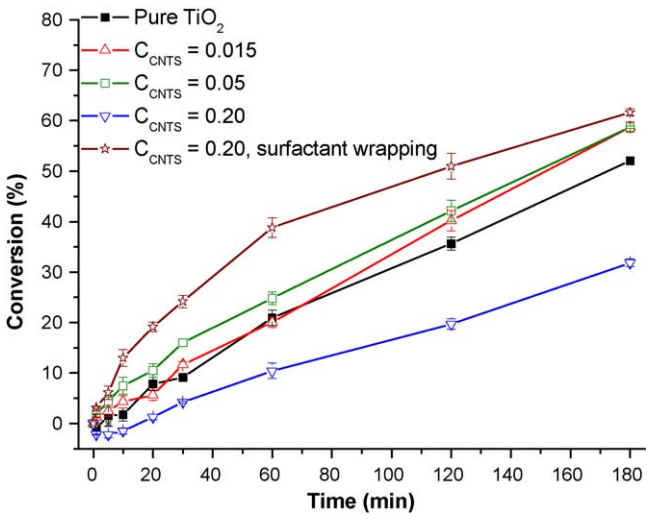

Fig. 6. Degradation of methylene blue in the presence of CNTs/TiO_2 nanocomposites with different carbon loadings, prepared by conventional and surfactant wrapping sol–gel methods. Irradiation started after 1 h dark adsorption–desorption equilibrium. Total catalyst loading = 0.1 g/L.

The results of this work compared favourably with those of Yu et al. [24], that reported 3% and 5% by weight as optimal CNTs/TiO_2 ratios for the decomposition of acetone in air, and Wang et al. [25] that reported 5% by weight to be an optimal CNTs/TiO_2 ratio for the degradation of 2,4-dinitrophenol. Yen et al. [26] described an enhancement of the degradation of phenol for CNTs/TiO_2 weight ratios up 8%, which contrasts with the work of Wang et al. [3] that suggested 20% to be the optimum CNTs/TiO_2 weight ratio for phenol degradation. Therefore, it appears that the optimum

loading of CNTs onto TiO_2 is a function of the target molecule being oxidised. However, this optimum should be found in the range from 1.5% to 20%.

The above findings apply to CNTs/TiO_2 nanocomposites prepared by conventional sol–gel methods. Conventional sol–gel methods usually lead to a heterogeneous, non-uniform coating of CNTs by TiO_2, showing bare CNTs surfaces and random aggregation of TiO_2 onto the CNTs surface.

3.4. Further enhancement of the oxidation rates with CNTs/TiO_2 nanocomposites prepared by the surfactant wrapping sol–gel method

The nanocomposites prepared by the surfactant wrapping sol–gel method, with acid pre-treatment of the CNTs, exhibited substantially higher photoactivities (15–20% higher) compared to the same materials prepared in the absence of acid pre-treatment of CNTs [27]. The experiments performed by varying the CNTs/TiO_2 ratio in the range 0–1.2, revealed that the nanocomposite with 0.2 weight ratio yielded the highest oxidation rate of methylene blue. The photocatalytic activity of this sample was evaluated under identical conditions as the samples prepared by the conventional sol–gel method in this work. Fig. 6 shows that the sample prepared by the surfactant wrapping sol–gel method exhibits a significant enhancement of the oxidation rate of methylene blue compared to the ones prepared by the conventional sol–gel approach. An enhancement of onefold of the initial rate was observed in comparison with the pure TiO_2. This level of rate enhancement is among the highest found in the literature for CNTs/TiO_2 nanocomposites photocatalytic oxidation of organic compounds in aqueous suspensions [28,29].

The significant level of rate enhancement by CNTs/TiO_2 nanocomposites prepared by the surfactant wrapping sol–gel method can be attributed to the improvement in the surface contact between the nanotubes and the metal oxide coating, which may compound with the other possible reasons for rate enhancement listed in Section 3.3. In contrast to the samples prepared by a conventional sol–gel method, the surfactant wrapping technique leads to uniform coating of the nanotubes by a thin TiO_2 layer of 5–10 nm in thickness [11], which does not show bare CNTs surfaces. This allows for optimal dispersion of the TiO_2 and optimal absorption of photons, since a much larger surface area of TiO_2 is exposed to photons either directly or by photon scattering within the suspension. The formation of a thin film of TiO_2 over the nanotubes should also contribute to a closer contact between the oxide layer and the nanotubes, with possible formation of heterojunctions. The absence of bare CNTs surfaces avoids losses of photons by absorption and scattering by the CNTs phase. The larger surface area ($S_{BET} = 295\ m^2/g$ before calcination, $V_{pore} = 0.245\ cm^2/g$) of these samples also may contribute towards an enhancement of the oxidation rate of methylene blue.

4. Conclusions

In this work, the conventional sol–gel method was used to prepare CNTs/TiO_2 nanocomposites with different carbon loadings. Based on the characterisation discussed above, the CNTs act as a dispersing agent in the composite system and induce synergistic effects on the catalytic properties. However, the photocatalytic rate enhancement with such materials was found to be limited and only available in a very narrow range of carbon content, up to 5% by weight. The random, heterogeneous assemblies of the TiO_2 nanoparticles on the tubular surfaces of CNTs are believed to be intrinsically responsible for the limited enhancement of the photocatalytic activity. The synthesis of CNTs/TiO_2 nanocomposites by the surfactant wrapping sol–gel method combined with CNTs pre-treatment led to nanocomposites that exhibited a significant enhancement of the oxidation rate of methylene blue. This larger degree of rate enhancement is attributed to the supporting role of the CNTs and surface properties prepared by this novel modified sol–gel method.

Acknowledgements

This work was supported by the University of Nottingham, Roberts Money, and partially from NATO grant CBP.EAP.SFPP 982835. We thank Mr. Yuxin Zhang and Prof. Huachun Zeng of the National University of Singapore and Dr. Chuang Peng from the University of Nottingham for their kind help in some experiments.

References

[1] S.-Y. Murakami, H. Kominami, Y. Kera, S. Ikeda, H. Noguchi, K. Uosaki, B. Ohtani, Res. Chem. Intermediat. 33 (2007) 285.
[2] C. Minero, D. Vione, Appl. Catal. B: Environ. 67 (2006) 257.
[3] W. Wang, P. Serp, P. Kalck, J.L. Faria, Appl. Catal. B: Environ. 56 (2005) 305.
[4] Y. Yu, J.C. Yu, C.-Y. Chan, Y.-K. Che, J.-C. Zhao, L. Ding, W.-K. Ge, P.-K. Wong, Appl. Catal. B: Environ. 61 (2005) 1.
[5] B. Ahmmad, Y. Kusumoto, S. Somekawa, M. Ikeda, Catal. Commun. 9 (2008) 1410.
[6] X.-H. Xia, Z.-J. Jia, Y. Yu, Y. Liang, Z. Wang, L.-L. Ma, Carbon 45 (2007) 717.
[7] T.Y. Lee, P.S. Alegaonkar, J.-B. Yoo, Thin Solid Films 515 (2007) 5131.
[8] M. Sánchez, R. Guirado, M.E. Rincón, J. Mater. Sci.: Mater. Electron. 18 (2007) 1131.
[9] H. Yu, X. Quan, S. Chen, H. Zhao, J. Phys. Chem. C 111 (2007) 12987.
[10] Y. Chen, J.C. Crittenden, S. Hackney, L. Sutter, D.W. Hand, Environ. Sci. Technol. 39 (2005) 1201.
[11] B. Gao, C. Peng, G.Z. Chen, G. Li Puma, Appl. Catal. B: Environ. 85 (2008) 17.
[12] G. Hu, X. Meng, X. Feng, Y. Ding, S. Zhang, M. Yang, J. Mater. Sci. 42 (2007) 7162.
[13] S. Aryal, C.K. Kim, K.-W. Kim, M.S. Khil, H.Y. Kim, Mater. Sci. Eng. C 28 (2008) 75.
[14] J. Cho, S. Schaab, J.A. Roether, A.R. Boccaccini, J. Nanopart. Res. 10 (2008) 99.
[15] K. Hernadi, E. Ljubović, J.W. Seo, L. Forró, Acta Mater. 51 (2003) 1447.
[16] J. Sun, L. Gao, M. Iwasa, Chem. Commun. 7 (2004) 832.
[17] A. Jitianu, T. Cacciaguerra, M.-H. Berger, R. Benoit, F. Béguin, S. Bonnamy, J. Non-Cryst. Solids 345–346 (2004) 596.
[18] A. Jitianu, T. Cacciaguerra, R. Benoit, S. Delpeux, F. Béguin, S. Bonnamy, Carbon 42 (2004) 1147.
[19] S.H.S. Zein, A.R. Boccaccini, Ind. Eng. Chem. Res. 47 (2008) 6598.
[20] M.S.P. Shaffer, X. Fan, A.H. Windle, Carbon 36 (1998) 1603.
[21] C. Peng, G.A. Snook, D.J. Fray, M.S.P. Shaffer, G.Z. Chen, Chem. Commun. 44 (2006) 4629.
[22] A. Kongkanand, P.V. Kamat, ACS Nano 1 (2007) 13.
[23] C. Lettmann, K. Hildenbrand, H. Kisch, W. Macyk, W.F. Maier, Appl. Catal. B: Environ. 32 (2001) 215.
[24] Y. Yu, J.C. Yu, J.-G. Yu, Y.-C. Kwok, Y.-K. Che, J.-C. Zhao, L. Ding, W.-K. Ge, P.-K. Wong, Appl. Catal. A: Gen. 289 (2005) 186.
[25] H. Wang, H.-L. Wang, W.-F. Jiang, Z.-Q. Li, Water Res. (2008), doi:10.1016/j.watres.2008.10.003.
[26] C.-Y. Yen, Y.-F. Lin, C.-H. Hung, Y.-H. Tseng, C.-C.M. Ma, M.-C. Chang, H. Shao, Nanotechnology 19 (2008) 045604–045611.
[27] B. Gao, Ph.D. Thesis, University of Nottingham, UK, 2008.
[28] B. Liu, H.C. Zeng, Chem. Mater. 20 (2008) 2711.
[29] H. Yu, X. Quan, S. Chen, H. Zhao, Y. Zhang, J. Photochem. Photobiol. A: Chem. 200 (2008) 301.